

Formation Flying Control in Eccentric Orbits

Michael Tillerson* and Jonathan P. How†
 Space Systems Laboratory
 Massachusetts Institute of Technology

Abstract

This paper extends recent work on the control of a formation of spacecraft orbiting about an eccentric reference orbit. The approach uses the equations for periodic relative motion that were previously developed from Lawden's original work. This paper presents fuel/time-optimal algorithms for the low-level station-keeping of one satellite with respect to another satellite in the presence of disturbances. The station-keeping algorithm is optimized by posing it as a linear programming problem. The primary extension of this paper is to present the solution to the linear programming problem using the time-varying linearized dynamics that occur for an eccentric reference orbit. Numerous nonlinear simulations were performed to demonstrate the effectiveness of this overall control approach. The results indicate that, even in the presence of differential J_2 disturbances, our formation flying control approach is very effective, requiring a $\Delta V = 5\text{--}15$ mm/s/orbit, depending on the scenario. The simulations also show that Lawden's equations are necessary for determining the desired state for periodic relative motion, but Hill's equations are sufficient for the linear programming control problem. This result is important because using the time-invariant Hill's equations significantly reduces the computational effort required to formulate the linear program.¹

Introduction

Many future space missions plan to use coordinated microsatellites to form a "virtual satellite bus" that replaces the standard monoliths used today [1]. To

achieve these future mission goals, several guidance, navigation, and control challenges must first be addressed. For example, very tight coordination, control, and monitoring of the distributed vehicles in the cluster will be required to achieve the stringent payload pointing requirements for a synthetic aperture radar mission, such as TechSat 21 [2]. Much of the research for cluster dynamic modeling and control has focused on the design of *passive apertures*, which are (short baseline) periodic formation configurations that provide good, distributed, Earth imaging while reducing the tendency of the vehicles to drift apart [3, 4, 6, 5].

Recent work in [6] presented passive apertures for eccentric orbits that were designed using the time-varying linearized dynamics first developed by Lawden [11, 12, 14, 15]. The results indicate that neglecting reference orbit eccentricity can lead to drift rates of meters per orbit, comparable to the effects of J_2 [6]. For example, the shuttle orbit has an eccentric orbit with $e \approx 0.005$, which results in 10's m/day drift depending on the formation baseline. This drift can be eliminated using the initial condition solution for eccentric orbits developed in Ref. [6]. However, disturbances such as differential drag, differential J_2 , etc. will continue to disturb the satellite from the desired periodic path.

This paper extends the convex optimization techniques presented in Ref. [8] to the time-varying linear dynamics of eccentric orbits. This step improves the model of the relative dynamics used in the control design, which should reduce the fuel costs associated with station-keeping. Using the satellite's current error from the desired state and the relative dynamics, the fuel optimal trajectory for returning to the desired state can be determined through the use of linear programming. Nonlinear simulations are performed to demonstrate the effectiveness of the

*Research Assistant, MIT Dept. of Aeronautics and Astronautics, mike_t@mit.edu

†Associate Professor, MIT Dept. of Aeronautics and Astronautics, jhow@mit.edu

¹Copyright © 2001 by the American Institute of Aeronautics and Astronautics, Inc. All rights reserved.

control method presented. The simulations display the fuel savings in using the time-varying dynamics of eccentric orbits instead of the approximations of Hill's equations. The simulations indicate the necessity of using Lawden's equations in determining the desired state for periodic relative motion in eccentric orbits. However, the results show that using Hill's equations in the linear programming control problem results in only a slight increase in fuel cost. This result is significant because using time-varying equations increases the computational effort required to formulate the linear program.

Relative Dynamics in Eccentric Orbits

The following section presents the dynamics for the relative motion of one satellite to a reference satellite on an eccentric orbit. A brief development of the equations of motion appears below, full details are available in Refs. [11, 12, 14, 15, 6].

Through kinematics the dynamics can be written in a non-inertial reference frame fixed on the formation center [6]. This frame orbits with the formation center. The coordinate system is defined with unit vectors, \hat{k}_x points radially outward from Earth's center and \hat{k}_y is in the intrack direction along increasing true anomaly. This right-handed reference frame is completed with \hat{k}_z , pointing in the out-of-track direction. The formation center, relative position of the satellite, and angular velocity of the orbit are expressed in the local frame as

$$\vec{\rho}_j = x_j \hat{k}_x + y_j \hat{k}_y + z_j \hat{k}_z \quad (1)$$

$$\vec{R}_{fc} = R_{fc} \hat{k}_x \quad \text{and} \quad \dot{\vec{\Theta}} = \dot{\theta} \hat{k}_z \quad (2)$$

The linearized relative dynamics of an eccentric orbit can be expressed in terms of relative states $[x_j, y_j, z_j]$ of each satellite, the radius, R_{fc} and the angular velocity, $\dot{\theta}$ of the formation center. Details of the linearization and change of coordinate system are in Refs. [6, 8]. From [9], the radius and angular velocity of the formation center are written as

$$|\vec{R}_{fc}| = \frac{a(1-e^2)}{1+e\cos\theta} \quad \text{and} \quad \dot{\theta} = \frac{n_o(1+e\cos\theta)^2}{(1-e^2)^{3/2}} \quad (3)$$

where $n_o = \sqrt{\mu/a^3}$ is the natural frequency of the reference orbit. With these expressions the relative dynamics in elliptic orbits can be written as a function of true anomaly, θ .

The homogenous solutions to the linear time-varying equations are available in literature for various reference frames and variables. The first derivation was provided by Lawden in 1963 [11] and similar results are available from Marec [12]. Carter [14, 15] removed the singularities in previous solutions and provides the basis of the solutions presented here. The solutions can be written in the time domain, but writing the equations as function of the true anomaly, θ , provides a more natural description. This is because both the radius of the orbit and angular velocity are functions of the true anomaly. The transition from time domain to θ -domain requires the following changes to the derivatives $(\dot{\cdot}) = (\cdot)'\dot{\theta}$; $(\ddot{\cdot}) = (\cdot)''\dot{\theta}^2 + \dot{\theta}\dot{\theta}'(\cdot)'$ [6]. The form presented in this paper also uses the following change of variables for position, $\vec{\rho}$, and velocity, $\vec{\rho}'$ [14].

$$\vec{\rho}_* = (1 + e \cos \theta) \vec{\rho}; \quad \vec{\rho}_*' = (1 + e \cos \theta) \vec{\rho}' - e \sin \theta \vec{\rho} \quad (4)$$

where $\vec{\rho} = (x, y, z)$ corresponds to the previous definition of the positions and $\vec{\rho}_* = (x_*, y_*, z_*)$ represents the transformed positions.

There is also a change in the reference frame. In this case, \hat{k}_{x*} is radially pointing, \hat{k}_{y*} is perpendicular to \hat{k}_{x*} , in the direction opposed to the motion, \hat{k}_{z*} remains out of plane and completes the \hat{k}_{y*} - \hat{k}_{x*} - \hat{k}_{z*} right hand coordinate frame. The homogenous solutions are now

$$\begin{aligned} x_*(\theta) &= r \sin \theta [b_1 e + 2b_2 e^2 H(\theta)] - \cos \theta \left[\frac{b_2 e}{r} + b_3 \right] \\ y_*(\theta) &= -r^2 [b_1 + 2b_2 e H(\theta)] - b_3 [1 + r] \sin \theta + b_4 \quad (5) \\ z_*(\theta) &= b_5 \cos \theta + b_6 \sin \theta \end{aligned}$$

$$\begin{aligned} x_*'(\theta) &= [\dot{r} \sin \theta + r \cos \theta] [b_1 e + 2b_2 e^2 H(\theta)] \\ &\quad + r \sin \theta [2b_2 e^2 \dot{H}(\theta)] + \sin \theta \left[\frac{b_2 e}{r} + b_3 r \right] \\ &\quad + \cos \theta \dot{r} \left[\frac{b_2 e}{r^2} - b_3 \right] \\ y_*'(\theta) &= -2r \dot{r} [b_1 + 2b_2 e H(\theta)] - r^2 [2b_2 e \dot{H}(\theta)] \\ &\quad - b_3 \dot{r} \sin \theta - b_3 [1 + r] \cos \theta \quad (6) \\ z_*'(\theta) &= -b_5 \sin \theta + b_6 \cos \theta \end{aligned}$$

The b_i 's are integration constants calculated from the corresponding initial conditions. The additional parameters in the solutions are $r = 1 + e \cos \theta$ and

$$\begin{aligned} H(\theta) &= \int_{\theta_0}^{\theta} \frac{\cos \theta}{(1 + e \cos \theta)^3} d\theta \\ &= -(1 - e^2)^{-5/2} \left[\frac{3eE}{2} - (1 + e^2) \sin E \right] \end{aligned}$$

$$+\frac{e}{2} \sin E \cos E + d_H] \quad (7)$$

$$\cos E = \frac{e + \cos \theta}{1 + e \cos \theta} \quad (8)$$

where E is the orbit eccentric anomaly and d_H is calculated from $H(\theta_0) = 0$.

Initialization

Previous work determined initial conditions for periodic motion in eccentric reference orbits for initial true anomaly, $\theta_0 = 0$ [6]. The initial conditions for periodic motion expressed in the θ -domain are

$$\frac{y'(0)}{x(0)} = -\frac{2+e}{1+e} \quad \text{or} \quad \frac{y'_*(0)}{x'_*(0)} = \frac{2+e}{1+e} \quad (9)$$

This condition provides a relationship between the initial radial position and in-track velocity for the spacecraft to maintain a periodic motion. Note this velocity is the true anomaly rate of change of the in-track position. The corresponding condition for the time-domain is

$$\frac{\dot{y}(0)}{x(0)} = -\frac{n(2+e)}{(1+e)^{1/2}(1-e)^{3/2}} \quad (10)$$

As $e \rightarrow 0$, Eq. 10 converges to the differential energy condition for Hill's equations, $\dot{y}(0)/x(0) = -2n$.

General Initialization

The initialization for periodic motion at other values of θ can also be obtained using Eqns. 5 and 6. For example, consider a spacecraft at some $\theta_d \neq 0$ with current values of the scaled position and velocities $x_*(\theta_d)$, $y_*(\theta_d)$, $x'_*(\theta_d)$, and $y'_*(\theta_d)$. Assuming that these values are not consistent with a periodic solution, they can be modified using Eq. 9. To start, first use Eqns. 5, 6 to define

$$\begin{bmatrix} x_*(\theta_d) \\ y_*(\theta_d) \\ x'_*(\theta_d) \\ y'_*(\theta_d) \end{bmatrix} = \begin{bmatrix} r_1 \\ r_2 \\ r_3 \\ r_4 \end{bmatrix} \begin{bmatrix} b_1 \\ b_2 \\ b_3 \\ b_4 \end{bmatrix} \equiv R B \quad (11)$$

$$\begin{bmatrix} x_*(0) \\ y'_*(0) \end{bmatrix} = \begin{bmatrix} r_{30} \\ r_{40} \end{bmatrix} B \quad (12)$$

where the r_i are the appropriate row vectors of coefficients for the b_i 's and r_{i0} is the row vector of coefficients evaluated at $\theta = 0$.

Eq. 9 constrains the relationship between $y'_*(0)$ and $x'_*(0)$ which can be rewritten as

$$\left(\frac{2+e}{1+e} r_{30} - r_{40} \right) B = 0 \quad (13)$$

Note the periodic constraint is equivalent to setting $b_2 = 0$. To complete the initialization, we assume that $x_*(\theta_d)$ and $y_*(\theta_d)$ must be the values provided previously and that only the values of $y'_*(\theta_d)$ and $x'_*(\theta_d)$ can be changed to achieve periodic motion. These assumptions provide three constraints on the four unknowns (the b_i 's). The fourth constraint can be developed in a variety of ways, depending on the factors that are most important.

Symmetric Motion For example, one approach would be to constrain the periodic motion so that it is symmetric in-track about the origin. Evaluating the $y_*(\theta)$ part of Eq. 5 at $\theta = 0$ and $\theta = \pi$ and setting the average to zero, yields the constraint

$$[-1 \quad -(1+e)H(0) + (1-e)H(\pi) \quad 0 \quad 1] B = 0 \quad (14)$$

Appending this constraint to the three given previously completely defines the periodic motion.

Fuel Optimal In general, the symmetric initialization requires that both $x'_*(\theta_d)$ and $y'_*(\theta_d)$ be modified, which can be fuel intensive. This naturally leads to the question of whether there is an optimal way to select the b_i 's that minimizes the fuel cost associated with changing $x'_*(\theta_d)$ and/or $y'_*(\theta_d)$ so that the four state values at θ_d are consistent with periodic motion. One solution to this problem is to pose it as an optimization that minimizes the ΔV required to obtain the initial velocities that are consistent with periodic relative motion at θ_d . Define the desired velocities for periodic motion $x'_{*}(\theta_d)_{\text{des}}$ and $y'_{*}(\theta_d)_{\text{des}}$ in terms of the initial velocities, $x'_{*}(\theta_d)_{\text{init}}$ and $y'_{*}(\theta_d)_{\text{init}}$, and the required incremental velocity changes, ΔV_x and ΔV_y as

$$\begin{aligned} x'_{*}(\theta_d)_{\text{des}} &= x'_{*}(\theta_d)_{\text{init}} + \Delta V_x \\ y'_{*}(\theta_d)_{\text{des}} &= y'_{*}(\theta_d)_{\text{init}} + \Delta V_y \end{aligned} \quad (15)$$

The $x'_*(\theta_d)$ and $y'_*(\theta_d)$ can be written in terms of the b_i (Eqn. 11) so the total ΔV can be expressed in terms of the knows and the b_i 's. Introducing the slack variables ΔV^+ and ΔV^- for each ΔV , the problem can be written as the linear program:

$$\begin{aligned} J &= \min c^T U \\ \text{subject to} \quad A_{\text{eq}} U &= b_{\text{eq}} \\ A_{\text{ineq}} U &\leq b_{\text{ineq}} \end{aligned} \quad (16)$$

where

$$\begin{aligned}
U^T &= \begin{bmatrix} \Delta V_x^+ & \Delta V_x^- & \Delta V_y^+ & \Delta V_y^- & b_1 & b_2 & b_3 & b_4 \end{bmatrix} \\
c^T &= \begin{bmatrix} 1 & 1 & 1 & 1 & 0 & 0 & 0 & 0 \end{bmatrix} \\
A_{\text{eq}} &= \begin{bmatrix} 1 & -1 & 0 & 0 & -r_3 & & & \\ 0 & 0 & 1 & -1 & -r_4 & & & \\ 0 & 0 & 0 & 0 & r_1 & & & \\ 0 & 0 & 0 & 0 & r_2 & & & \\ 0 & 0 & 0 & 0 & \frac{2+\epsilon}{1+\epsilon}r_{30} - r_{40} & & & \end{bmatrix} \\
b_{\text{eq}} &= \begin{bmatrix} -x'_*(\theta_d)_{\text{init}} \\ -y'_*(\theta_d)_{\text{init}} \\ x_*(\theta_d) \\ y_*(\theta_d) \\ 0 \end{bmatrix}
\end{aligned}$$

and A_{ineq} is an 4×8 matrix of zeros with $A_{11} = A_{22} = A_{33} = A_{44} = -1$ and b_{ineq} is an 4×1 vector of zeros. These inequality constraints force the slack variables to be positive. The LP problem has four variables and nine constraints. The equality constraint satisfies the position constraints in Eqn. 11, the velocity constraints in Eqn. 15, and the periodicity constraint in Eqn. 13. The solution of the LP problem contains the four b_i 's and the Δv 's required to change the initial velocities to the desired velocities for periodic motion.

The LP problem was tested on many different cases, and the solution always resulted in only a change in the in-track velocity to meet the periodicity constraint. The radial velocity remained unchanged from the (potentially random) initial value that was provided to the problem. This suggests the following simple alternative solution.

Velocity Constraint The final formulation simply imposes the constraint that the radial velocity not change from the initial value provided. Thus $x_*(\theta_d)$, $y_*(\theta_d)$, $x'_*(\theta_d)$ must be the values provided previously and only $y'_*(\theta_d)$ can be changed by the initialization process. The periodicity constraint in Eq. 13 then provides the fourth constraint:

$$\begin{bmatrix} x(\theta_d)' \\ y(\theta_d)' \\ v_x(\theta_d)' \\ 0 \end{bmatrix} = \begin{bmatrix} r_1 \\ r_2 \\ r_3 \\ (\frac{2+\epsilon}{1+\epsilon}r_{30} - r_{40}) \end{bmatrix} B \equiv \tilde{R} B$$

In this case the constants of integration in the prob-

lem are given by

$$B = \tilde{R}^{-1} \begin{bmatrix} x_*(\theta_d) \\ y_*(\theta_d) \\ x'_*(\theta_d) \\ 0 \end{bmatrix}$$

which then completely defines the initialization process for any value of θ

Examples Sample initializations and resulting trajectories are presented in Figs. 1 and 2. The initializations were determined for $\theta_d = 5^\circ$ and $\theta_d = 45^\circ$. The \circ represents the given initial position. Using the initial conditions determined by the LP initialization approach, the trajectory was propagated for four orbits. Note that there was no noticeable drift in either example. As is clearly shown for the case initialized at $\theta_d = 45^\circ$, the periodic motion is no longer centered about the reference orbit $(0, 0)$.

LP Trajectory Planning and Control

A linear programming trajectory planning approach has recently been developed to design fuel-optimized trajectories and station-keeping control inputs using Hill's equations [8]. This section extends and applies this approach to the time-varying dynamics of eccentric orbits.

The linear time-varying dynamics can be compactly written in the form

$$\dot{x} = A(\theta)x(\theta) + B(\theta)u(\theta) + B_d(\theta)w(\theta) \quad (17)$$

where the inputs are now divided into control inputs u and disturbance inputs w . The dynamics can then be discretized using the sampling period, T_s . With the inclusion of the desired output and the direct transition matrices, the discrete relative dynamics take the following form [10] ($t = kT_s$)

$$\begin{aligned}
x(k+1) &= \Phi_k x(k) + \Gamma_k u(k) + M_k w(k) \\
y(k) &= H_k x(k) + J_k u(k) + P_k w(k) \quad (18)
\end{aligned}$$

where $x(k) \in R^n$ are the states, $u(k) \in R^m$ are control inputs, and $w(k) \in R^p$ are the disturbances acting on the system. The vector $y(k) \in R^l$ are the measured outputs or the variables of interest to the control design. The output $y(k)$ can be calculated using discrete convolution of the form (for $k \geq 1$)

$$y(k) = H_k \Phi^{(k,k)} x(0) + [J_k u(k) + P_k w(k)]$$

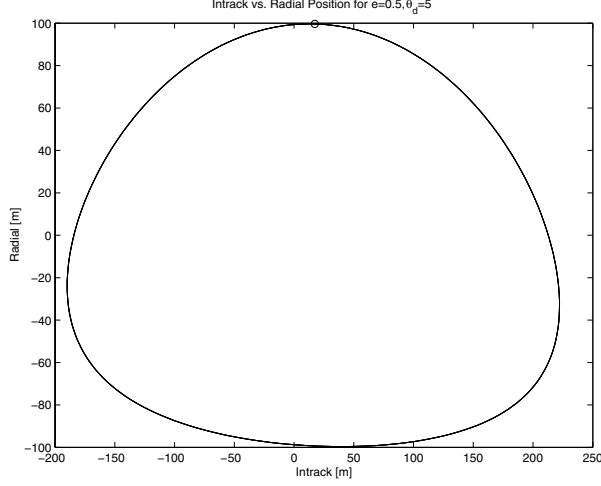


Fig. 1: Trajectory followed for 4 orbits using initialization at $\theta_d = 5^\circ$. The \circ represents the initial constrained position.

$$+ \sum_{i=0}^{k-1} H_k \Phi^{(k-i-1,k)} [\Gamma_i u(i) + M_i w(i)] \quad (19)$$

where $\Phi^{(j,k)}$ corresponds to

$$\Phi^{(j,k)} = \begin{cases} \Phi^{(k-1)} \cdots \Phi^{(k-j+1)} \Phi^{(k-j)} & 2 \leq j \leq k \\ \Phi^{(k-1)} & j = 1 \\ I & j = 0 \end{cases}$$

Note that if the fleet has a circular reference orbit, then the system matrices ($\Phi_k, \Gamma_k, H_k, J_k, M_k, P_k$) will be independent of time and $\Phi^{(k-i-1,k)}$ simply corresponds to Φ^{k-i-1} . Eq. 19 has the simple matrix representation

$$y(k) = A(k)U_k + b(k) \quad (20)$$

$$A(k) = [H_k \Phi^{(k-1,k)} \Gamma_0, \dots, H_k \Phi^{(0,k)} \Gamma_{k-1} \quad J_k] \quad (21)$$

$$b(k) = [H_k \Phi^{(k-1,k)} M_0, \dots, H_k \Phi^{(0,k)} M_{k-1}, P_k] \begin{bmatrix} w(0) \\ w(1) \\ \vdots \\ w(k) \end{bmatrix} + H_k \Phi^{(k,k)} x(0) \quad (22)$$

where $H_k \Phi^{(k-1,k)} \Gamma_0$ is the pulse response of the system which maps the inputs

$$U_k = [u(0)^T \quad u(1)^T \quad \dots \quad u(k-1)^T \quad u(k)^T]^T \quad (23)$$

to the output observed at the k^{th} step.

This plant description, Eq. 20, is the basis of the trajectory and control design using LP. Note that in

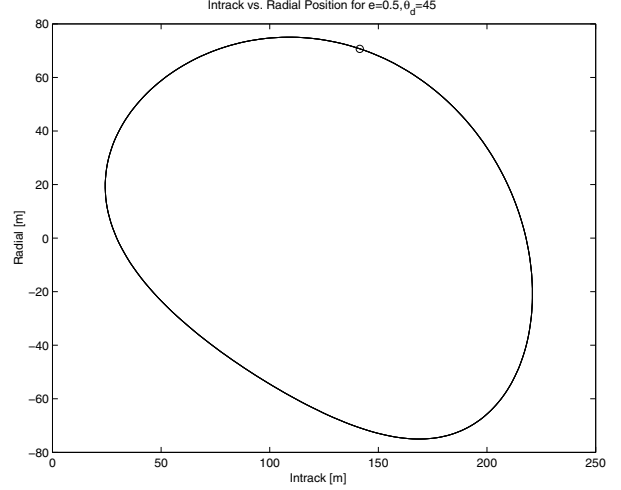


Fig. 2: Trajectory followed for 4 orbits using initialization at $\theta_d = 45^\circ$. The \circ represents the initial constrained position.

this case, the index k corresponds to steps in the true anomaly. We find the solution as a function of k and then convert back to the time domain for implementation in the simulations to follow. The conversion from true anomaly to time is straight forward using the relation between true anomaly and eccentric anomaly

$$\tan \frac{E}{2} = \left[\frac{1-e}{1+e} \right]^{1/2} \tan \frac{\theta}{2} \quad (24)$$

and then using Kepler's Equation to solve for the time

$$\sqrt{\frac{\mu}{a^3}}(t - \tau) = E - e \sin E \quad (25)$$

The only additional required information is the time of perigee passage τ .

The general LP problem is to control the spacecraft to a desired terminal relative state after n steps in true anomaly, while minimizing a weighted sum ($c_j \geq 0$) of the $\|\cdot\|_1$ norm of the control inputs by each spacecraft. This standard control problem is given by

$$\min_{U_n} \sum_{j=1}^m c_j \|u_j\|_1 \quad \text{subject to } y_{\text{des}}(n) = A(n)U_n + b(n)$$

where $u_j = [u_j(0) \quad u_j(1) \quad \dots \quad u_j(n)]^T$ is the fuel used by the j^{th} actuator on the spacecraft. To rewrite this problem as a linear program, two slack variables are introduced that define the positive and negative

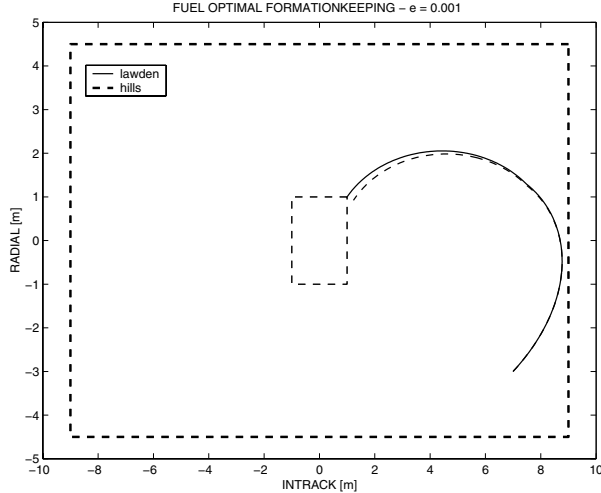


Fig. 3: Trajectories designed using Lawden's and Hill's equations – reference orbit $e = 0.001$ and half-orbit plan time. Final position error ≈ 0.2 m.

parts of the control input

$$U_n = U_n^+ - U_n^-, \quad U_n^+ \geq 0, \quad U_n^- \geq 0 \quad (26)$$

Using c_{ij} as the weight for the input from the j^{th} actuator at the i^{th} time step, define

$$C^T = [c_{00} \ c_{01} \ \dots \ c_{nm} \ c_{00} \ c_{01} \ \dots \ c_{nm}]$$

as the weights on each of the positive and negative parts of the control inputs. The standard problem can then be rewritten as the linear program [13]

$$J_{\text{sp-lp}}^* = \min_{\hat{U}_n} C^T \hat{U}_n \quad (27)$$

subject to

$$\begin{bmatrix} A(n) & -A(n) \end{bmatrix} \hat{U}_n = y_{\text{des}}(n) - b(n)$$

As given in the structure of the problem, the information necessary to complete the control problem are the initial state x_0 , the desired goal $y_{\text{des}}(n)$, and the system limitations embedded in the inequality constraints. The LP determines the control inputs for a specified span of true anomaly (time interval) that minimizes the fuel cost, the sum of the inputs, while satisfying the constraints on the trajectory.

Additional constraints to the problem can include: state constraints such as remaining within some tolerance of a specified point defined by an error box, maximum input values (actuator saturation), actuator rate limits, etc. This approach can also include differential disturbances such as drag

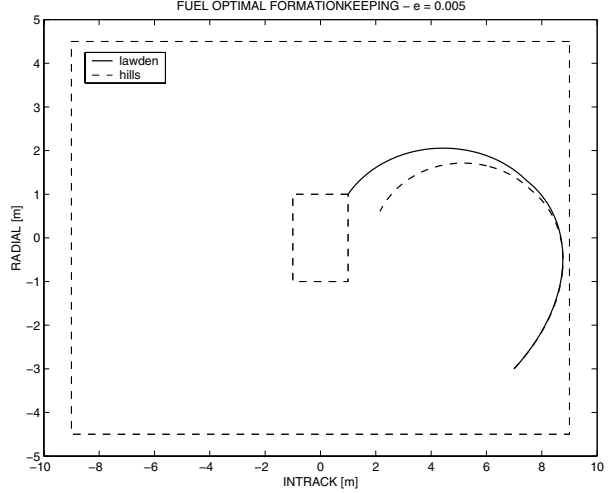


Fig. 4: Trajectories designed using Lawden's and Hill's equations – reference orbit $e = 0.005$ and half-orbit plan time. Final position error ≈ 2.2 m.

and linearized forms of the differential J_2 effects (see Ref. [3] for details on these models). Methods of adding these additional constraints and disturbances are included in Ref. [8]. To complete the low-level control design for station-keeping, the LP is embedded within a real-time optimization control approach that monitors the spacecraft relative positions and velocities, and then redesigns the control input sequence if the vehicle approaches the edge of the error box or a new terminal state is desired [8].

Sample trajectories generated using LP for Lawden's Equations are shown in Figure 3 and Figure 4. for eccentricity values of $e = 0.001$ and $e = 0.005$. Some of the constraints included are: (1) the vehicle positions must remain within the error box at all times, (2) the final position must be within 1 m of the center of the box, and (3) the actuator inputs must not exceed the limits. The trajectories followed using inputs designed using Hill's equations are also plotted for comparison. For eccentricity of 0.001 the error in using a circular orbit reference (i.e. Hill's equations) results in a final position error of approximately 0.2 m. For eccentricity = 0.005 the final position error is ≈ 2 m.

Simulations

Several nonlinear simulations were performed using FreeFlyerTM orbit simulator [7] in order to demonstrate the effectiveness of the LP control method

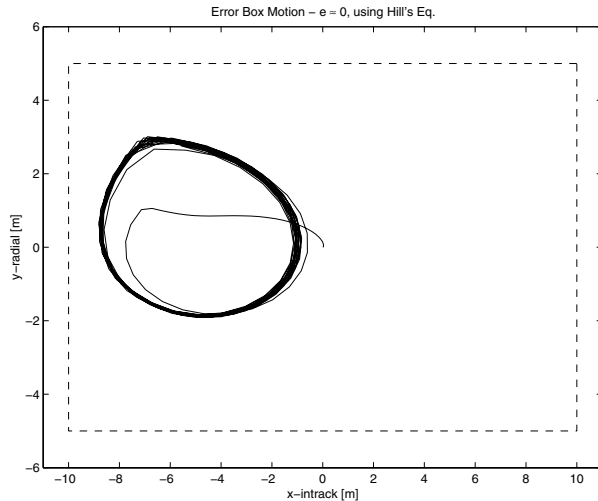


Fig. 5: Error Box motion for a reference orbit with $e \approx 0$, using Hill's Equations. The average fuel cost was 6.548 mm/s/orbit.

and determine the effect of eccentricity error on the fuel use for satellite station-keeping. The simulations have two satellites with a 100 m separation that are initialized for periodic motion using Eq. 9 or Eq. 10. The FreeFlyerTM orbit simulator propagates the absolute states of both satellites. The simulator allows the option of including or excluding disturbances such as drag, lift, solar radiation pressure, and J_2 . The simulator software interfaces with MATLABTM, which is where the control calculations are performed.

The states of the two satellite are first converted from the ECI frame to the local reference frame described earlier. The desired relative state of the second satellite is then determined based on the formation center's (the other satellite in the simulations) true anomaly, eccentricity, and semi-major axis. These calculations use the homogenous solutions to the relative dynamics in Eqs. 5 and 6. This desired relative state is differenced with the satellites true relative state to give the current *error state*. An *error box* is centered on the desired position and used to determine if control action is required. The size of the error box is determined by the position tolerances permitted for the mission objective. Based on the position tolerance of 10% of the baseline (100 m) specified by the TechSat 21 mission objectives [2], a 10 m in-track, 5 m radial, and 5 m out-of-plane box is used in these simulations. If the relative position of the satellites approaches the edge of the error box,

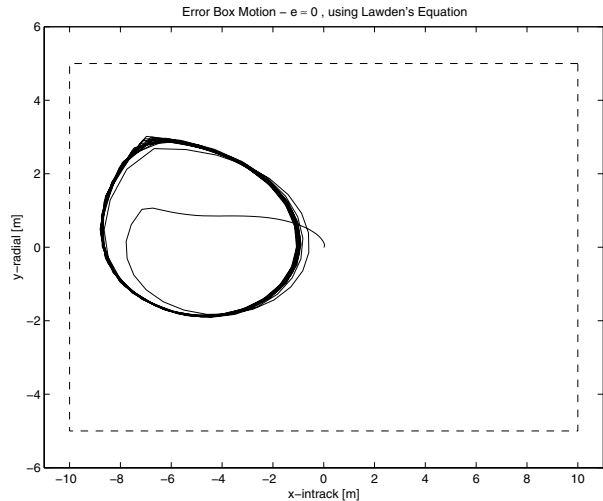


Fig. 6: Error Box motion for a reference orbit with $e \approx 0$, using Lawden's Equations. The average fuel cost was 6.530 mm/s/orbit.

then the control inputs are calculated (using an LP) to determine the fuel optimal trajectory and control inputs to return the satellite to the center of the error box in a specified time interval. During maneuvers, the satellite thrusters are restricted to provide a maximum acceleration of 0.003 m/s^2 and a minimum of $5 \times 10^{-6} \text{ m/s}^2$. The maximum thrust corresponds to turning on the thruster for the full time step. The minimum thrust is determined from a minimum impulse bit of 10 msec during the time step. The control inputs, if required, are converted to small displacements and velocity changes using the time changing dynamics. These relative state variables are transformed back to the ECI frame and are added to the absolute state vector of the satellite after the force-free propagation is performed by the FreeFlyerTM software. The result is a real-time linear control in a nonlinear simulation environment.

Simulation #1 : Figures 5 - 9

The first group of simulations demonstrate the effectiveness of the control using Lawden's time varying equations of motion and the corresponding conditions for periodic motion in eccentric orbits. The satellites are in an approximately 90 minute orbit and the eccentricity is increased from 0 to 0.01. The same simulations were performed once using Hill's equations of motion and corresponding initial conditions and once using Lawden's equations of motion and initial conditions to show how the error in as-

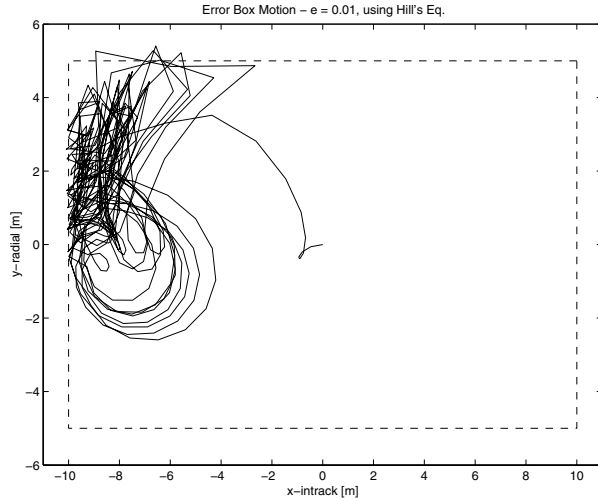


Fig. 7: Error Box motion for a reference orbit with $e = 0.01$, using Hill's Equations. The average fuel cost was 107.5 mm/s/orbit.

suming a circular orbit effects the efficiency of the control and increases the fuel cost.

In order to clearly examine the effect of eccentricity modeling error on the LP control and fuel use for station keeping, only the differential drag disturbances are implemented in the FreeFlyerTM simulation, other disturbances such as J_2 effects and solar radiation pressure are not implemented. The J_2 and other disturbances are disabled in the FreeFlyerTM simulations because the dynamics in the LP do not account for these disturbances. J_2 also effects the eccentricity which would cause an additional disturbance to the controller which is not the focus of these simulations. For each simulation, the satellite begins in the center of the error box and drifts to the edge due to a differential drag. When the satellite nears the edge, a series of control inputs are determined that would move the satellite to within 1 m of the center of the error box and reduce the velocity error to within 0.5 mm/s. The LP plan interval is half an orbit (45 min) and the satellite is constrained to remain inside the error box during the plan interval.

Figures 5 and 6 show the motion of the satellite within the error box for a reference orbit with $e \approx 0$. There is little difference between the two, which is as would be expected (in the limit as $e \rightarrow 0$, Lawden's equations return to Hill's equations). The fuel cost is also approximately the same (6.548 mm/s/orbit using Hill's and 6.530 mm/s/orbit using Lawden's).

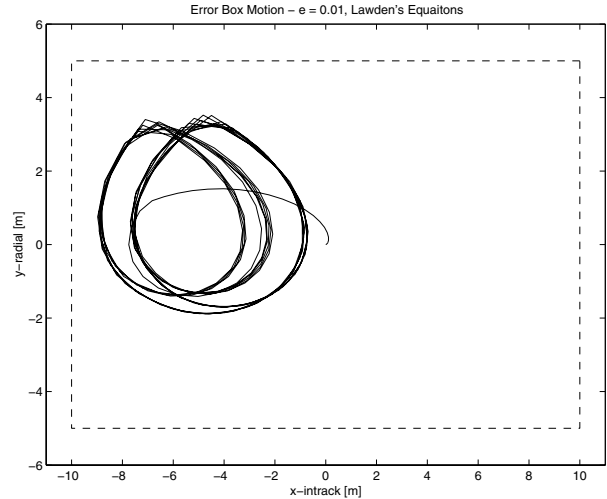


Fig. 8: Error Box motion for a reference orbit with $e = 0.01$, using Lawden's Equations. The average fuel cost was 9.481 mm/s/orbit.

The fuel cost includes fuel used in the radial, intrack, and crosstrack directions, however the crosstrack fuel cost was zero for this simulation. Figures 7 and 8 show the error box motion for a reference orbit with $e = 0.01$. The fuel cost was 107.5 mm/s per orbit using Hill's and 9.481 mm/s per orbit using Lawden's equations, which is a drastic difference. Again, the crosstrack fuel cost was zero. Clearly Hill's equations are no longer appropriate because the orbit is not circular, and this is confirmed by the inability of the control to return the satellite to the center of the error box. However, Lawden's equations are still effective. The difference in motion between Figure 6 and Figure 8 is due to the difference in drag in an elliptical orbit. For the case $e = 0$, a constant model for the drag is reasonable because the altitude of the satellite does not vary much. For $e > 0$ the altitude varies, so the drag in the simulation is not constant. An improved model of the drag could be implemented in the LP to correct this error. The fuel cost versus eccentricity is summarized in Figure 9. The three cases included in the plot are:

1. Use Hill's initial conditions to determine the desired state for periodic motion and Hill's equations of motion for the LP.
2. Use Lawden's initial conditions to determine the desired state, but use Hill's equations of motion in the LP, and
3. Use Lawden's initial conditions to determine

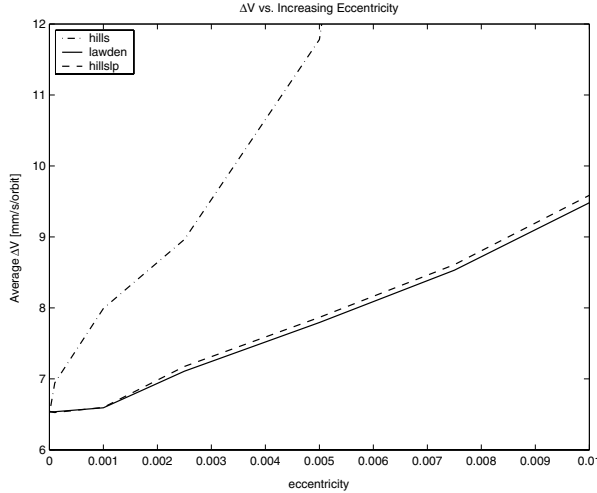


Fig. 9: ΔV fuel cost versus increasing eccentricity for control using the three (IC and model) cases described in the text.

desired state and Lawden’s equations of motion for the LP.

As shown in the plot, using Hill’s initial conditions to determine the desired state leads to an increased fuel cost, even for very small values of the reference orbit eccentricity. However, these results also indicate that using Hill’s equations in the LP does not significantly increase the fuel cost much if e is small ($e < 0.01$). This observation is important because the LP using Lawden’s equations requires a discretization of the time-varying dynamics at every step in true anomaly considered in the LP. This tends to dramatically increase the amount of computation required to set up the LP optimization, although the LP size does not change, so computation time for solving the LP does not increase. With Hill’s equations, the matrices are constant and need only be formed once. However as the eccentricity becomes larger, the trajectories designed using Hill’s in the LP becomes less effective and the fuel cost will be larger than the LP using Lawden’s dynamics. This was demonstrated in Figures 3, 4.

Simulation #2 : Table 1

To further examine the difference between using Lawden’s versus Hill’s dynamics in the LP, simulations were performed with increasing plan horizon in the LP. A reference orbit with $e = 0.005$ was used in these simulations. Table 1 contains average fuel costs for increasing plan horizons using Lawden’s and Hill’s

equations. The fuel cost using either form of dynamics decreases with increasing plan horizon because the longer plan time allows smaller control inputs and takes advantage of the nonlinear motion to increase “drift” time between control inputs. Using Hill’s equations rather than Lawden’s results in only a slight increase in fuel cost as the plan horizon increases. The time-invariant Hill’s equations, however, result in decreased computation time in the LP formulation as mentioned before. The increase in fuel cost for Hill’s is due to using control inputs based on dynamics with errors that add up at each time step.

Table 1: ΔV for increasing plan horizon.

Time (orbits)	0.5	0.75	1.0	1.25
Hill’s	7.969	3.723	2.109	1.701
Lawden’s	7.746	3.416	1.751	1.543

Simulation #3 : Figures 10- 13

To test the true performance of the controller, the following simulations include all disturbances, differential drag, lift, solar radiation pressure, J_2 , etc. The duration of the simulation is two days which is long enough to observe the effects of J_2 on the controller. The disturbance effects are set for what is believed to be a worst case scenario in that the drift due to differential drag and the drift due to J_2 are in the same direction. The differential drag could be set such that the drift partially cancels the drift due to J_2 , however this was not done in the following simulations. The controller uses Lawden’s equations for desired state determination as well as for the dynamics in the LP. The first simulation is for a reference orbit with $e = 0.005$. The average fuel cost is 8.241 mm/s/orbit. This fuel cost includes the cost to control the crosstrack perturbations caused by J_2 . Using Lawden’s equations results in only a slight increase in fuel cost with all disturbances included. The motion of the satellite within the error box is shown in Figure 10 and the fuel cost is shown in Figure 11. For comparison, control using Hill’s equations results in a fuel cost of ≈ 300 mm/s/orbit, which is clearly not acceptable.

A simulation with $e = 0.5$ was also performed. For the orbit to be feasible the semi-major axis was increased to 14000 km, which results in ≈ 275 minute orbit. The error box motion is shown in Figure 12

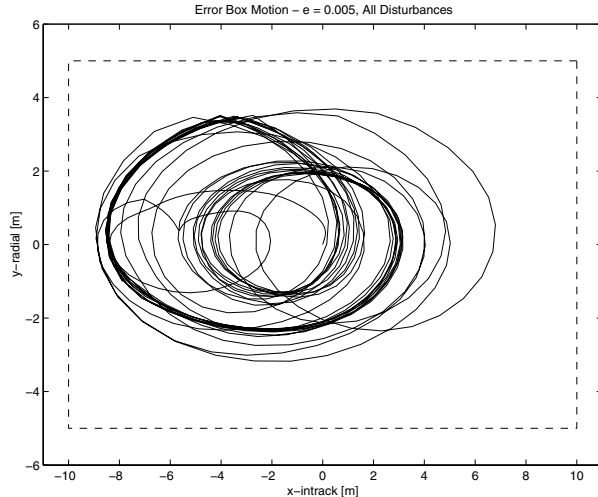


Fig. 10: Error box motion with all disturbances included for a reference orbit $e = 0.005$.

and the average fuel cost was 11.812 mm/s per orbit. The fuel cost is plotted in Figure 13.

These simulations show that even in the presence of J_2 , the control is effective. J_2 causes short and long period oscillations in the eccentricity [16]. For low eccentricity these oscillations dominate and are on the order of 0.001 which was shown earlier to cause an increase in fuel cost when using Hill's instead of Lawden's equations of motion. By using Lawden's equations in the LP formulation, the osculating eccentricity could easily be included in the dynamics for the trajectory planning, capturing some of the effects of J_2 in the dynamics.

Conclusions

Formation flying is an enabling technology for many future science missions. Previous work has focused on the design and control of passive apertures based on a circular reference orbit. Extending the design and control to eccentric orbits provides many new advantages. Operation advantages include longer operating times in particular regions of interest and increased useful observation time by decreasing the occlusion time of the Earth.

This paper presents the relative dynamics of satellites in eccentric orbits as well as conditions for periodic motion in these orbits. The paper extends the LP control strategy from the time-invariant linearized relative equations of motion for circular reference orbits to the time-varying equations of motion

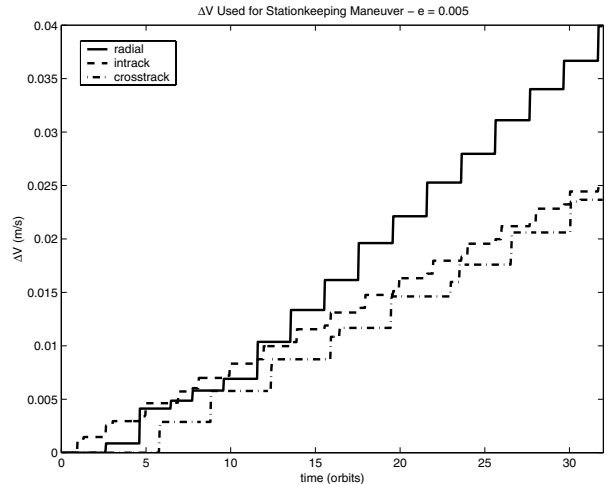


Fig. 11: ΔV fuel cost with all disturbances included for a reference orbit $e = 0.005$. The average fuel cost is 8.241 mm/s/orbit.

for eccentric orbits. The control design was tested using nonlinear simulations. The simulations show an increased fuel cost when assuming a circular reference orbit for an actual reference orbit with eccentricity as low as 0.001. The key to successful control in eccentric orbits is in the determination of the desired state to maintain periodic motion. Using Hill's equations to determine the desired state results in controlling to a state that does not result in periodic motion thus drastically increasing fuel cost. Further reduction in fuel cost can be achieved by including the time-varying dynamics in the LP control determination, however this increases computation time in the formulation of the LP. The control was successfully demonstrated for orbit eccentricities from ≈ 0 to 0.5 with all disturbances included (differential drag, lift, solar radiation pressure, J_2) with only a small increase in fuel cost.

Acknowledgments

Research funded under Air Force grant #F49620-99-1-0095 and NASA GSFC grant #NAG5-6233-0005. Special thanks to Gokhan Inalhan at Stanford University for his numerous discussions.

References

- [1] J. How, R. Twiggs, D. Weidow, K. Hartman, and F. Bauer, "Orion: A low-cost demonstration of formation flying in space using GPS," in *AIAA Astrodynamics Specialists Conf.*, Aug 1998.

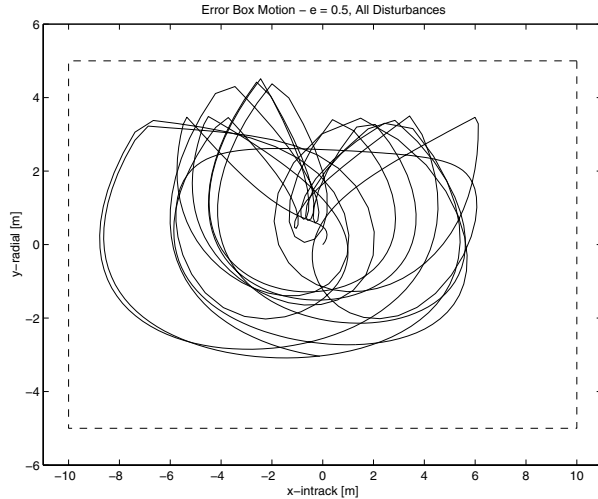


Fig. 12: Error box motion with all disturbance included for a reference orbit $e = 0.5$. Semi-major axis 14000 km.

- [2] Air Force Research Laboratory Space Vehicles Directorate, “TechSat 21 factsheet page.” <http://www.vs.afrl.af.mil/factsheets/TechSat21.html>.
- [3] R. J. Sedwick, D. W. Miller and E. M. Kong, “Mitigation of Differential Perturbations in Synthetic Apertures Comprised of Formation Flying Satellites”, presented at the 9th AAS/AIAA Space Flight Mechanics Meeting, February 7-10, 1999.
- [4] H. Yeh, A. Sparks, “Geometry and Control of Satellite Formations,” in Proc. of 2000 ACC, (Chicago, IL), June 2000.
- [5] K. T. Alfriend, H. Schaub, and D.-W. Gim, “Gravitational Perturbations, Nonlinearity and Circular Orbit Assumption Effects on Formation Flying Control Strategies,” Vol. 104, *Advances in the Astronautical Sciences, Guidance and Control* p. 139.
- [6] G. Inalhan, and How, J. P., “Relative Dynamics & Control of Spacecraft Formations in Eccentric Orbits,” presented at the AIAA GN&C Conference, Aug 2000.
- [7] A.I. Solutions, “FreeFlyer User’s Guide”, Version 4.0, March 1999.
- [8] M. Tillerson, G. Inalhan, and J. How, “Coordination and Control of Distributed Spacecraft Systems Using Convex Optimization Techniques,” submitted to the *International Journal of Robust and Non-linear Control*, Nov. 2000.
- [9] V. A. Chobotov, “Orbital Mechanics,” Second Edition, AIAA Educational Series, 1996.
- [10] G. F. Franklin, J. D. Powell, M. Workman, “Digital Control of Dynamic Systems,” Third Edition, Addison-Wesley, 1998.
- [11] D. F. Lawden, “Optimal Trajectories for Space Navigation,” Butterworths, London, 1963.

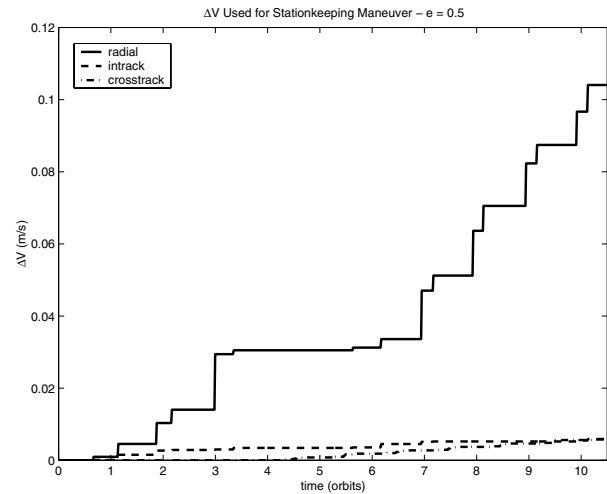


Fig. 13: ΔV fuel cost with all disturbance included for a reference orbit $e = 0.5$. Semi-major axis 14000 km. The average fuel cost is 11.812 mm/s/orbit.

- [12] J.P. Marec, “Optimal Space Trajectories,” Elsevier Scientific, NY 1979
- [13] S. Boyd, L. Vanderberghe, “Convex Optimization,” *Manuscript form*, www.stanford.edu/class/ee364/reader.ps, 1999.
- [14] T. E. Carter and M. Humi, “Fuel-Optimal Rendezvous Near a Point in General Keplerian Orbit,” *J. of Guidance, Control and Dynamics*, Vol. 10 No. 6, Nov.-Dec. 1987
- [15] T. E. Carter, “New Form for the Optimal Rendezvous Equations Near a Keplerian Orbit,” *Journal of Guidance, Control and Dynamics*, Vol. 13 No. 1, Jan-Feb 1990
- [16] D. A. Vallado. *Fundamentals of Astrodynamics and Applications*. McGraw-Hill, 1997.